The Astrophysical Journal, 825:70 (15pp), 2016 July 1 doi:10.3847/0004-637X/825/1/70

ORBITAL EVOLUTION OF MASS-TRANSFERRING ECCENTRIC BINARY SYSTEMS. I. PHASE-DEPENDENT EVOLUTION

Fani Dosopoulou and Vicky Kalogera
Center for Interdisciplinary Exploration and Research in Astrophysics (CIERA) and Department of Physics and Astrophysics, Northwestern University, Evanston, IL 60208, USA; FaniDosopoulou2012@u.northwestern.edu
Received 2016 March 20; revised 2016 April 21; accepted 2016 April 24; published 2016 June 29

ABSTRACT

Observations reveal that mass-transferring binary systems may have non-zero orbital eccentricities. The time evolution of the orbital semimajor axis and eccentricity of mass-transferring eccentric binary systems is an important part of binary evolution theory and has been widely studied. However, various different approaches to and assumptions on the subject have made the literature difficult to comprehend and comparisons between different orbital element time evolution equations not easy to make. Consequently, no self-consistent treatment of this phase has ever been included in binary population synthesis codes. In this paper, we present a general formalism to derive the time evolution equations of the binary orbital elements, treating mass loss and mass transfer as perturbations of the general two-body problem. We present the self-consistent form of the perturbing acceleration and phase-dependent time evolution equations for the orbital elements under different mass loss/transfer processes. First, we study the cases of isotropic and anisotropic wind mass loss. Then, we proceed with non-isotropic ejection and accretion in a conservative as well as a non-conservative manner for both point masses and extended bodies. We compare the derived equations with similar work in the literature and explain the existing discrepancies.

Key words: binaries: close – binaries: general – planets and satellites: dynamical evolution and stability – stars: kinematics and dynamics – stars: mass-loss – X-rays: binaries

1. INTRODUCTION

In modeling binary populations, most interacting mass-transferring binary systems are assumed to be circular (e.g., Belczynski et al. 2008). However, observations reveal that semi-detached binary systems might have non-zero orbital eccentricities (e.g., Petrova & Orlov 1999; Bonačić Marinović et al. 2008; Vos et al. 2013; Boffin et al. 2014). In addition, recent observations indicate that high-mass X-ray binaries (HMXB) are eccentric, with relatively high eccentricities in the case of Be/X-ray binaries (e.g., Raguzova & Popov 2005; Walter et al. 2015). The residual eccentricity that has been observed in mass-transferring binary systems is quite surprising, since tidal dissipation might be expected to circularize the orbit and drive the star toward co-rotation (e.g., Hut 1981; Eggleton et al. 1998; Bonačić Marinović et al. 2008). This implies that the efficiency of tidal circularization in interacting eccentric binaries is not as high as is typically assumed. Previous work has shown that, especially for long-period systems and solar-type binaries in open clusters, tides are not sufficient to circularize the orbit, thus leaving the systems with a considerable non-zero eccentricity (e.g., Meibom & Mathieu 2005; Vos et al. 2012, 2013, 2015). Mass loss and mass transfer processes have been proposed as possible mechanisms to help the system retain a finite eccentricity.

Mass loss/transfer can indeed enhance eccentricity (e.g., Soker 2000; Bonačić Marinović et al. 2008; Vos et al. 2015) and is a common evolutionary phase in a binary system, being responsible for many observed astrophysical phenomena such as SNe Ia, X-ray binaries, neutron-star spin up, as well as orbital contraction or expansion. Mass can be ejected or accreted in a binary system in many different and complicated ways and is phase-dependent in an eccentric orbit. Commonly studied cases include isotropic wind mass loss (e.g., Hadjidemetriou 1963), Roche-lobe-overflow (RLOF; e.g., Sepinsky et al. 2007, 2009), and Bondi–Hoyle accretion (e.g., Bondi & Hoyle 1944; Boffin & Jorissen 1988; Hurley et al. 2002). All of the aforementioned processes change the total mass, energy, and orbital angular momentum of the binary, which correspond to a change in the binary orbital elements. The effect of mass transfer on the orbital elements has long been studied (e.g., Huang 1956; Hadjidemetriou 1963) and continues to be a subject of interest with recent work studying various different cases of mass loss and mass transfer (e.g., Sepinsky et al. 2007, 2009, 2010; Veras et al. 2011, 2013).

In the existing literature, to our knowledge, the time evolution of the orbital elements of a binary undergoing mass loss and mass transfer has been derived by following two different approaches. One approach involves calculating the time variations of the orbital elements based on changes in the total orbital energy and angular momentum of the system (e.g., Huang 1956; Boffin & Jorissen 1988; Bonačić Marinović et al. 2008). The other method involves treating mass loss/transfer as a perturbation in the two-body problem and using the latter to calculate the time evolution of the orbital elements (e.g., Hadjidemetriou 1963; Sepinsky et al. 2009; Veras et al. 2011, 2013). However, consistency between these two different approaches is not always clear and many assumptions that have implicitly been made following either technique are not always clearly stated. Thus, having a general mathematical formalism to describe the orbital evolution of a binary system undergoing various types of mass transfer is both useful and important in binary evolution theory. In the first part of this paper, we demonstrate how to derive the time evolution equations of the orbital elements based on the Lagrange perturbation formalism, and then apply this to specific cases of mass loss and mass transfer in eccentric binaries.

A binary system exposed to different kinds of perturbations follows an orbit that is continuously evolving in time, i.e., an open orbit. This means that much attention must be paid to the

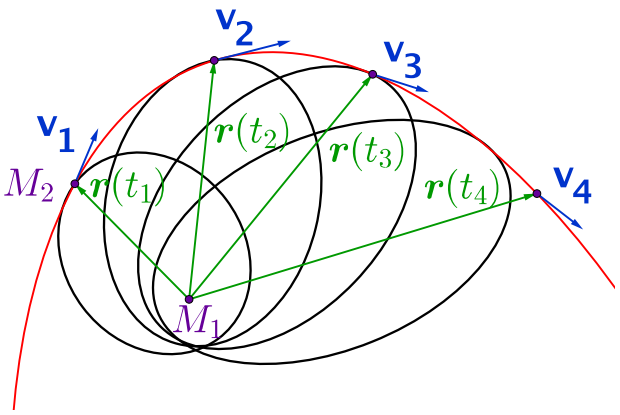

Figure 1. Definition of osculating elements. The instantaneous conics are always tangential to the perturbed actual physical orbit of the body.

physical interpretation of the orbital elements we assign to the evolving orbit (e.g., Efroimsky & Goldreich 2004; Veras et al. 2011). In this work, we refer to the importance of this interpretation, which is connected both to the freedom in the choice of orbital elements and the gauge freedom in orbital mechanics.

The paper is organized as follows. In Section 2, we present the general formalism we use to describe the perturbed two-body problem. In Section 3, we comment on the importance of the choice of reference frame and present the time evolution equations of the orbital elements in three different reference frames. In Sections 4 and 5, we apply this formalism to the cases of isotropic and anisotropic wind mass loss, respectively. In Section 6, we study conservative as well as non-conservative non-isotropic mass ejection and accretion in the system for extended binary components. In Section 7, we present the form that the time evolution equations of the orbital elements reduce to under the point-mass approximation. Throughout all of the aforementioned sections, we present comparisons to previous work in the literature for similar cases. Finally, an explanation of any existing discrepancies is provided. In Section 8, we summarize our results.

The perturbing acceleration is in principle phase-dependent. In this paper, we present the general form of the perturbing acceleration and the orbital element time evolution equations, keeping this phase-dependence. In a follow-up paper, Dosopoulou & Kalogera (2016; hereafter Paper II), we orbit-average the phase-dependent time evolution equations of the orbital elements relevant to different types of mass loss/transfer in the binary under either the assumption of adiabaticity or for delta-function mass loss/transfer at periastron.

2. THE PERTURBED TWO-BODY PROBLEM

Two-body systems like binary stars can be exposed to gravitational perturbations from different agents. These agents include tidal dissipation, relativistic corrections, gravitational-wave radiation, magnetic fields, inertial forces, mass loss/mass transfer phenomena, and others. All of these physical processes act as perturbing forces on the general two-body problem and require a new mathematical way of treatment compared to the unperturbed case. Due to the various perturbations, each body is no longer moving in the actual physical trajectory (conic section) it would be if no perturbations existed, but its physical orbit is slowly changing with time.

Referred to as either *Variation of constants* in pure mathematical language or the *Varying-Conic method* in purely geometric terms, the method that was proposed to study these systems was advanced and completed by Lagrange. This method involves an approximation of the true physical orbit by a family of evolving instantaneous conic sections.

In Section 2.1, we will prove that the latter representation is not unique, and thus one should be very meticulous when applying this mathematical formulation. Specifically, the actual physical orbit of the body is open and the orbital elements derived through this method are not the classic orbital elements of a closed orbit. Rather, they either can have a possible physical interpretation under certain assumptions or they should be treated just as mathematical tools otherwise. We will discuss this issue in more detail in the following sections.

2.1. Variation of Constants Method

The general reduced two-body problem is described by the equation

$$\ddot{\boldsymbol{r}} = -\frac{GM}{r^3}\boldsymbol{r}, \tag{1}$$

where G is the gravitational constant, M is the total mass of the system, and r is the relative position between the two bodies. The general solution to this problem is a Keplerian conic section defined by six constant orbital elements $\{C_i\} = \{C_1, \ldots, C_6\}$.

In a specified inertial coordinate system, this conic is described by

$$\boldsymbol{r} = \boldsymbol{r}(C_1, \ldots, C_6, t), \quad \dot{\boldsymbol{r}} = (C_1, \ldots, C_6, t), \tag{2}$$

where, by definition,

$$\boldsymbol{v} = \left(\frac{\partial \boldsymbol{r}}{\partial t}\right)_{C_i=\text{const.}} \tag{3}$$

is the relative velocity between the two bodies in the system.

The *perturbed* two-body problem can then be written as

$$\ddot{\boldsymbol{r}} = -\frac{GM}{r^3}\boldsymbol{r} + \boldsymbol{F}(\boldsymbol{r}, \dot{\boldsymbol{r}}), \tag{4}$$

where the perturbing force $\boldsymbol{F}(\boldsymbol{r}, \dot{\boldsymbol{r}})$ depends on both the relative position and velocity.

Equation (4) can be solved by assuming that at each instant of time, the true orbit can be approximated by an instantaneous Keplerian Conic section which is changing over time through the now *time-dependent* orbital elements C_i, i.e.,

$$\boldsymbol{r} = \boldsymbol{r}(C_1(t), \ldots, C_6(t), t), \tag{5}$$

and the velocity of the body will now be given by

$$\dot{\boldsymbol{r}} = \frac{\partial \boldsymbol{r}}{\partial t} + \sum_{i=1}^{6} \frac{\partial \boldsymbol{r}}{\partial C_i}\frac{dC_i}{dt}. \tag{6}$$

Equations (4) and (6) constitute a system of three independent equations, one independent variable (time t), and six dependent variables (orbital elements $C_i(t)$). This means that the parametrization in terms of the orbital elements is not unique and additional constraints need to be applied.

2.1.1. Lagrange Constraint—Osculating Elements

Imposing the *Lagrange constraint*

$$\sum_{i=1}^{6}\frac{\partial \boldsymbol{r}}{\partial C_i}\frac{dC_i}{dt}=0 \tag{7}$$

makes the orbital elements $C_i(t)$ *osculating*. This means that the instantaneous conics are tangential to the perturbed actual physical orbit, as can be seen with Equation (7) and as depicted in Figure 1.

Another way to think about osculating orbits is that these are the orbits that the body would follow if perturbations were to cease instantaneously.

Equations (4), (6), and (7) constitute a now well-defined system of six equations and six variables.

Following the Lagrange constraint, the perturbed equation of motion (4) can be written as

$$\frac{\partial^2 \boldsymbol{r}}{\partial t^2}+\frac{GM}{r^3}\boldsymbol{r}+\sum_{i=1}^{6}\frac{\partial \boldsymbol{v}}{\partial C_i}\frac{dC_i}{dt}=\boldsymbol{F}, \tag{8}$$

where $\boldsymbol{r}$ refers to the solution of the unperturbed two-body problem, i.e., satisfies Equation (1).

This simplifies Equation (8) to

$$\sum_{i=1}^{6}\frac{\partial \boldsymbol{v}}{\partial C_i}\frac{dC_i}{dt}=\boldsymbol{F}, \tag{9}$$

which, using the definition of Lagrange and Poisson brackets, can be decoupled to read

$$\frac{dC_i}{dt}=-\sum_{j=1}^{6}\{C_iC_j\}\frac{\partial \boldsymbol{r}}{\partial C_j}\boldsymbol{F}. \tag{10}$$

Poisson brackets are defined by

$$\{C_kC_i\}=\frac{\partial C_k}{\partial \boldsymbol{r}}\frac{\partial C_i}{\partial \boldsymbol{v}}-\frac{\partial C_k}{\partial \boldsymbol{v}}\frac{\partial C_i}{\partial \boldsymbol{r}}, \tag{11}$$

they are the negative inverse to Lagrange brackets

$$[C_kC_i]=\frac{\partial \boldsymbol{r}}{\partial C_k}\frac{\partial \boldsymbol{v}}{\partial C_i}-\frac{\partial \boldsymbol{r}}{\partial C_i}\frac{\partial \boldsymbol{v}}{\partial C_k}, \tag{12}$$

and do not depend on time explicitly.

Equation (10) gives the time evolution equations of the six osculating orbital elements, which are invariant with respect to the change of coordinates and/or orbital parametrization.

We choose the six Keplerian elements (a, e, i, Ω, ω, ν), namely, semimajor axis, eccentricity, inclination, argument of periapsis, longitude of the ascending node, and true anomaly ν. Also, we define $n=(GM/a^3)^{1/2}$ as the mean motion.

Making use of the following Poisson brackets,

$$\{\sigma a\}=-\{a\sigma\}=\frac{2}{na} \tag{13}$$

$$\{\sigma e\}=\frac{1-e^2}{na^2e},\ \{\omega e\}=-\frac{\sqrt{1-e^2}}{na^2e} \tag{14}$$

$$\{\sigma a\}=-\frac{\sqrt{1-e^2}}{na^2e} \tag{15}$$

$$\{\Omega i\}=-\frac{1}{na^2\sqrt{1-e^2}\sin i} \tag{16}$$

$$\{\omega i\}=-\frac{\cos i}{na^2\sqrt{1-e^2}\sin i}, \tag{17}$$

yields the following Lagrange time evolution equations for the aforementioned six orbital elements:

$$\frac{da}{dt}=\frac{2}{na}\boldsymbol{F}\frac{\partial \boldsymbol{r}}{\partial \sigma} \tag{18}$$

$$\frac{de}{dt}=\frac{1-e^2}{na^2e}\boldsymbol{F}\frac{\partial \boldsymbol{r}}{\partial \sigma}-\frac{\sqrt{1-e^2}}{na^2e}\boldsymbol{F}\frac{\partial \boldsymbol{r}}{\partial \omega} \tag{19}$$

$$\frac{di}{dt}=\frac{1}{na^2\sqrt{1-e^2}\sin i}\left[\cos i\ \ \boldsymbol{F}\frac{\partial \boldsymbol{r}}{\partial \omega}-\boldsymbol{F}\frac{\partial \boldsymbol{r}}{\partial \Omega}\right] \tag{20}$$

$$\frac{d\omega}{dt}=\frac{\sqrt{1-e^2}}{na^2e}\boldsymbol{F}\frac{\partial \boldsymbol{r}}{\partial e}-\frac{\cos i}{na^2\sqrt{1-e^2}\sin i}\boldsymbol{F}\frac{\partial \boldsymbol{r}}{\partial i} \tag{21}$$

$$\frac{d\Omega}{dt}=\frac{1}{na^2\sqrt{1-e^2}\sin i}\boldsymbol{F}\frac{\partial \boldsymbol{r}}{\partial i} \tag{22}$$

$$\frac{d\nu}{dt}=\frac{n(1+e\cos\nu)^2}{(1-e^2)^{3/2}}-\frac{d\omega}{dt}-\cos i\frac{d\Omega}{dt}. \tag{23}$$

We note here that the orbital elements appearing in Equations (18)–(23) are, as we will explain in detail in the following sections, the so-called *osculating elements*. The physical meaning of these elements as well as their uniqueness with respect to any other choice of orbital elements will also be explained in the next sections.

Equations (18)–(23) describe the time evolution of all six orbital elements. Since we are interested only in perturbations induced by mass loss/transfer processes, and for reasons we describe in detail in the last paragraph of the following section, in this paper we present only the time evolution of the semimajor axis a and the eccentricity e (see Equations (18) and (19)). However, as we can see from Equations (21)–(23), for a general perturbation the orbit undergoes various precessions. At the end of the following section, we also briefly discuss these precessions. In Paper II, we discuss in more detail the importance of these precessions within the context of secular evolution.

2.1.2. Introducing Gauge Freedom in Orbital Mechanics—Non-osculating Elements

According to Efroimsky & Goldreich (2004), imposing the Lagrange constraint is not necessary and one is free to set

$$\sum_{i=1}^{6}\frac{\partial \boldsymbol{r}}{\partial C_i}\frac{dC_i}{dt}=\boldsymbol{\Phi}, \tag{24}$$

where $\boldsymbol{\Phi}$ is called *the gauge* and represents the gauge freedom in orbital mechanics.

Further generalizing the formulation by writing the perturbing force $\boldsymbol{F}$ in terms of a perturbing Lagrangian,

$$\boldsymbol{F}=\frac{\partial \Delta L}{\partial \boldsymbol{r}}-\frac{d}{dt}\left(\frac{\partial \Delta L}{\partial \dot{\boldsymbol{r}}}\right), \tag{25}$$

one can re-write Equations (18) and (19) as follows (e.g., Efroimsky & Goldreich 2004):

$$\frac{da}{dt} = \frac{2}{na}\left[\frac{\partial(-\Delta H)}{\partial\sigma} - \frac{\partial\Delta L}{\partial\dot{\boldsymbol{r}}}\frac{\partial}{\partial\sigma}\left(\boldsymbol{\Phi} + \frac{\partial\Delta L}{\partial\dot{\boldsymbol{r}}}\right) - \left(\boldsymbol{\Phi} + \frac{\partial\Delta L}{\partial\dot{\boldsymbol{r}}}\right)\frac{\partial\boldsymbol{g}}{\partial\sigma} - \frac{\partial\boldsymbol{f}}{\partial\sigma}\frac{d}{dt}\left(\boldsymbol{\Phi} + \frac{\partial\Delta L}{\partial\dot{\boldsymbol{r}}}\right)\right] \quad (26)$$

$$\frac{de}{dt} = \frac{1-e^2}{na^2e}\left[\frac{\partial(-\Delta H)}{\partial\sigma} - \frac{\partial\Delta L}{\partial\dot{\boldsymbol{r}}}\frac{\partial}{\partial a}\left(\boldsymbol{\Phi} + \frac{\partial\Delta L}{\partial\dot{\boldsymbol{r}}}\right) - \left(\boldsymbol{\Phi} + \frac{\partial\Delta L}{\partial\dot{\boldsymbol{r}}}\right)\frac{\partial\boldsymbol{g}}{\partial\sigma} - \frac{\partial\boldsymbol{f}}{\partial\sigma}\frac{d}{dt}\left(\boldsymbol{\Phi} + \frac{\partial\Delta L}{\partial\dot{\boldsymbol{r}}}\right)\right] - \frac{\sqrt{1-e^2}}{na^2e}\left[\frac{\partial(-\Delta H)}{\partial\omega} - \frac{\partial\Delta L}{\partial\dot{\boldsymbol{r}}}\frac{\partial}{\partial\omega}\left(\boldsymbol{\Phi} + \frac{\partial\Delta L}{\partial\dot{\boldsymbol{r}}}\right) - \left(\boldsymbol{\Phi} + \frac{\partial\Delta L}{\partial\dot{\boldsymbol{r}}}\right)\frac{\partial\boldsymbol{g}}{\partial\omega} - \frac{\partial\boldsymbol{f}}{\partial\omega}\frac{d}{dt}\left(\boldsymbol{\Phi} + \frac{\partial\Delta L}{\partial\dot{\boldsymbol{r}}}\right)\right], \quad (27)$$

where ΔH is the perturbing Hamiltonian defined by

$$\Delta H = -\left[\Delta L + \frac{1}{2}\left(\frac{\partial\Delta L}{\partial\dot{\boldsymbol{r}}}\right)^2\right] \quad (28)$$

and the functions $\boldsymbol{f}$ and $\boldsymbol{g}$ have the same functional form as the unperturbed-case position and velocity vector, but are now time-dependent through the time-dependent orbital elements C_i. We note here that Equation (27) seems to have a singularity in the case of circular orbits ($e = 0$). This singularity is not real since to take the limit of Equation (27) for $e \to 0$, one first needs to calculate explicitly the form of the partial derivatives included in this equation as functions of the orbital elements.

For a general gauge $\boldsymbol{\Phi}$, they are connected to the perturbed velocity and position by the relations

$$\boldsymbol{r} = \boldsymbol{f}(C_1, \ldots, C_6, t) \quad (29)$$

$$\dot{\boldsymbol{r}} = \frac{\partial\boldsymbol{f}}{\partial t} + \boldsymbol{\Phi} \quad (30)$$

$$= \boldsymbol{g} + \boldsymbol{\Phi}. \quad (31)$$

Equations (30) and (31) constitute a physical interpretation of the gauge freedom.

Choosing the Lagrange constraint $\boldsymbol{\Phi} = 0$, one enforces the family of the approximating conics to be always tangent to the physical orbit of the body. In other words, this means that the orbital elements under this constraint are osculating elements and describe the conic the body would follow if the perturbation ceased instantaneously.

Any other non-zero constraint $\boldsymbol{\Phi}$ would lead to orbital elements that do not describe conics that are tangential to the real orbit, but differ from the tangent velocity vector by $\boldsymbol{\Phi}$ (see Figure 2). These elements are the so-called *non-osculating* elements and can be used in some cases as useful mathematical tools to describe the problem (e.g., Efroimsky 2002).

It is obvious that a real physical interpretation can be assigned only to the osculating elements (Lagrange constraint), since only those describe conics that are tangent to the actual path of the body at any time.

We should point out here that even the osculating orbital elements derived by this formulation are mathematical tools that can be used approximately to describe the real trajectory of the body. This means that one should be very meticulous when interpreting them. The physical time evolution of the system is precisely expressed with the time derivative of the position vector of the body $\dot{\boldsymbol{r}}$.

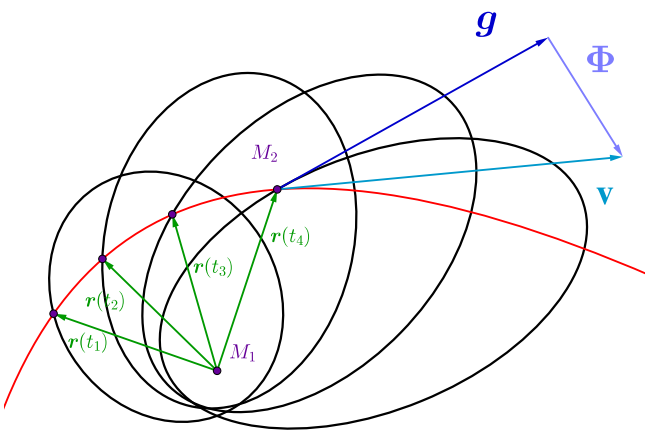

Figure 2. Definition of non-osculating elements. The tangent velocity $\boldsymbol{g}$ to the instantaneous conics differs from the tangent velocity vector to the actual physical orbit of the body $\boldsymbol{v} = \dot{\boldsymbol{r}}$ by the gauge $\boldsymbol{\Phi}$. The latter introduces the gauge freedom in orbital mechanics.

The time evolution equations for the osculating orbital elements include periodic terms that describe the natural oscillations these elements undergo due to the periodicity of the orbit. When the change in the orbital elements over one orbit is small, then an orbit-averaged method can be adopted to smooth out these oscillations leading to the secular (orbit-averaged) osculating orbital elements. In addition, if the perturbation timescale is much longer than the orbital timescale, then these secular time evolution equations can be resolved into a simpler form. The regime where a perturbation is changing slowly throughout the orbit so that it can be considered constant over an orbit (i.e., an "adiabatic invariant") is called the adiabatic regime. In this regime, the "adiabatic" secular time evolution equations for the osculating orbital elements are valid. When the orbital period becomes gradually comparable to the perturbation timescale, then adiabaticity is broken and the "adiabatic" secular time evolution equations no longer apply. Veras et al. (2011) studied the oscillations of the osculating orbital elements in the case of mass loss in the adiabatic regime as well as in the regime following the breaking of adiabaticity.

When applying Equations (18) and (19), or alternatively (26) and (27), to any kind of problem, one needs to know the various partial derivatives of $\boldsymbol{f}$ and $\boldsymbol{g}$ with respect to the orbital elements. For this reason, we calculated and present in the Appendix all of the required mathematical quantities as functions of the true anomaly ν.

Before proceeding to the application of the aforementioned zero-gauge and gauge-free formulations to specific physical problems, we would like to comment on the usefulness and advantages of each of them.

Based on what we presented here, there are two ways one can derive the time evolution equations of the orbital elements. One way is by using the perturbing force $\boldsymbol{F}$ directly applying the osculating Equations (18) and (19), and the other way is by using the equivalent Lagrangian ΔL defined by Equation (25) and applying Equations (26) and (27). Although these two different approaches are completely equivalent, eventually

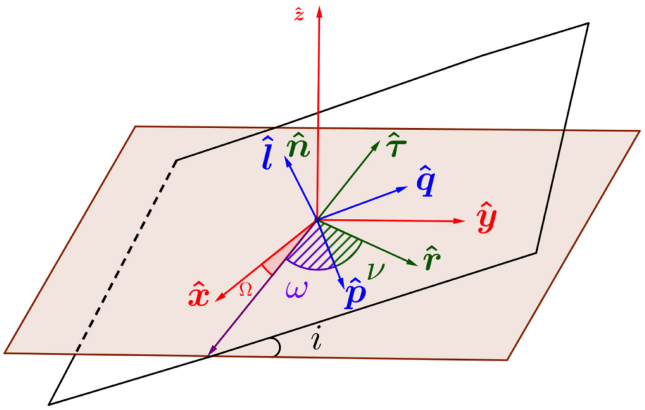

Figure 3. Definition of different reference frames. Solid shaped planes and angles refer to the inertial reference frame ($\hat{x}$, $\hat{y}$, $\hat{z}$), while hatch-shaped angles refer to the orbital plane inclined by angle i. In the latter, two reference systems are defined. The reference system ($\hat{p}$, $\hat{q}$, $\hat{l}$) where the unit vector $\hat{p}$ always points in the direction of periastron and ω is the argument of periapsis, and the reference system ($\hat{r}$, $\hat{\tau}$, $\hat{n}$), which is rotated by the true anomaly ν relative to the former.

leading to the same equations for the osculating orbital elements, the second method which makes use of the Lagrangian is more general because it introduces the gauge freedom. This means that the latter is the only method one could use to choose a gauge different than zero. There are cases where the use of a gauge other than zero is needed, e.g., when the Delaunay variables need to remain canonical for a general perturbation depending both on the positions and velocities of the bodies (e.g., Efroimsky & Goldreich 2003, 2004).

In the next sections, we will apply the gauge-free method to derive and compare the orbital element time evolution equations between a zero-gauge and a different gauge $\boldsymbol{\Phi}$, called the *generalized Lagrange constraint*, which is commonly used in the literature (e.g., Efroimsky 2002; Gurfil & Belyanin 2008) and is defined by

$$\boldsymbol{\Phi} = -\frac{\partial \Delta L}{\partial \dot{\boldsymbol{r}}}. \tag{32}$$

Using this gauge in Equations (26) and (27) gives the time evolution equations of the so-called *contact* orbital elements. As mentioned above, although Equations (26) and (27) are simplified by using this gauge, the derived contact orbital elements have no physical meaning compared to the zero-gauge and the relevant osculating orbital elements.

3. THE IMPORTANCE OF REFERENCE FRAME CHOICE

It is important to note that Equations (18) and (19) are in vector form, and are thus independent of the reference frame used in each specific problem. After decomposing the perturbing force $\boldsymbol{F}$ in these equations into its components in a chosen reference frame, one should be careful when interpreting the resulting equations for the semimajor axis and the eccentricity. In this section, we discuss the importance of the reference frame choice, pointing out that a vanishing component of the perturbing force in one specific reference frame does not guarantee any other vanishing component of the perturbing force in a different reference frame (see the rotation matrices (48)–(50)).

The most commonly used reference frames K_I, K_J, K_R to describe a two-body problem are depicted in Figure 3. The reference system $K_I(\hat{x}, \hat{y}, \hat{z})$ is the inertial reference system. In the reference system $K_J(\hat{p}, \hat{q}, \hat{l})$, the unit vector $\hat{p}$ is along the eccentricity vector and always points in the direction of periastron (rotated by the two angles i and ω relative to K_I). Finally, in the reference system $K_R(\hat{r}, \hat{\tau}, \hat{n})$, the unit vector $\hat{r}$ is along the relative position vector between the two bodies in the binary (rotated relative to K_J by the angle of true anomaly ν).

Acceleration $\boldsymbol{A}$ can be written in these reference frames as follows:

$$\boldsymbol{A} = A_x\hat{\boldsymbol{x}} + A_y\hat{\boldsymbol{y}} + A_z\hat{\boldsymbol{z}} \tag{33}$$

$$\boldsymbol{A} = A_p\hat{\boldsymbol{p}} + A_q\hat{\boldsymbol{q}} + A_l\hat{\boldsymbol{l}} \tag{34}$$

$$\boldsymbol{A} = A_r\hat{\boldsymbol{r}} + A_\tau\hat{\boldsymbol{\tau}} + A_n\hat{\boldsymbol{z}}. \tag{35}$$

The form of Equations (18) and (19) will be different based on the reference frame chosen each time in the problem. The use of the correct set of equations for the chosen reference frame is important because using the incorrect set of equations can lead to misinterpretation of the system's orbital evolution. Here, we present this set of equations for three different refernce frames.

For decomposition (33) in the reference system $K_I(\hat{x}, \hat{y}, \hat{z})$, Equations (18) and (19) take the form

$$\left(\frac{da}{dt}\right)_{\hat{x},\hat{y},\hat{z}} = \frac{2}{n\sqrt{1-e^2}}[\{C_1\cos i\sin\Omega + C_2\cos\Omega\}A_x - \{C_1\cos i\cos\Omega - C_2\sin\Omega\}A_y - \{C_1\sin i\}A_z] \tag{36}$$

$$\left(\frac{de}{dt}\right)_{\hat{x},\hat{y},\hat{z}} = \frac{\sqrt{1-e^2}}{2an(1+e\cos\nu)}[\{C_6\cos i\sin\Omega + C_5\cos\Omega\}A_x - \{C_6\cos i\cos\Omega - C_5\sin\Omega\}A_y - \{C_6\sin i\}A_z], \tag{37}$$

where the different C_i are defined by

$$C_1 = e\cos\omega + \cos(\nu+\omega) \tag{38}$$

$$C_2 = e\sin\omega + \sin(\nu+\omega) \tag{39}$$

$$C_5 = (2e\cos\nu + 1 + \cos^2\nu)\sin\omega \tag{40}$$

$$+2(e+\cos\nu)\cos\omega\sin\nu \tag{41}$$

$$C_6 = (2e\cos\nu + 1 + \cos^2\nu)\cos\omega \tag{42}$$

$$-2(e+\cos\nu)\sin\omega\sin\nu. \tag{43}$$

For decomposition (34) in the reference system $K_J(\hat{p}, \hat{q}, \hat{l})$, Equations (18) and (19) become

$$\left(\frac{da}{dt}\right)_{\hat{p},\hat{q},\hat{l}} = \frac{2}{n\sqrt{1-e^2}}[-A_p\sin\nu + A_q(e+\cos\nu)] \tag{44}$$

$$\left(\frac{de}{dt}\right)_{\hat{p},\hat{q},\hat{l}} = \frac{\sqrt{1-e^2}}{na(1+e\cos\nu)}[-A_p\sin\nu(e+\cos\nu) + A_q(2e\cos\nu + 1 + \cos^2\nu)]. \tag{45}$$

For decomposition (35) in the reference system $K_R(\hat{r}, \hat{\tau}, \hat{n})$, Equations (18) and (19) yield

$$\left(\frac{da}{dt}\right)_{\hat{r},\hat{\tau},\hat{n}} = \frac{2}{n\sqrt{1-e^2}}[A_r e\sin\nu + A_\tau(1+e\cos\nu)] \tag{46}$$

$$\left(\frac{de}{dt}\right)_{\hat{r},\hat{\tau},\hat{n}} = \frac{(1-e^2)^{1/2}}{na}\left[A_r \sin\nu + A_\tau \frac{2\cos\nu + e(1+\cos^2\nu)}{1+e\cos\nu}\right]. \quad (47)$$

Transformation between the different reference systems is done using the appropriate rotation matrices. Specifically, the cyclic transformation $K_I \rightarrow K_J \rightarrow K_R$ is performed using the relations

$$Q^T K_I \rightarrow K_J \quad (48)$$

$$RK_J \rightarrow K_R \quad (49)$$

$$Q^T K_I \rightarrow K_R,\ \omega \rightarrow \omega + \nu, \quad (50)$$

where the right arrow in Equation (50) means substituting ω with $\omega + \nu$ in the rotation matrix Q^T. The rotation matrices $\boldsymbol{Q}$ and $\boldsymbol{R}$ are defined by

$$\boldsymbol{Q} = \begin{pmatrix} Q_{11} & Q_{12} & Q_{13} \\ Q_{21} & Q_{22} & Q_{23} \\ Q_{31} & Q_{32} & Q_{33} \end{pmatrix} \quad (51)$$

and

$$Q_{11} = \cos\Omega\cos\omega - \sin\Omega\sin\omega\cos i \quad (52)$$

$$Q_{12} = -\cos\Omega\sin\omega - \sin\Omega\cos\omega\cos i \quad (53)$$

$$Q_{13} = \sin\Omega\sin i \quad (54)$$

$$Q_{21} = \sin\Omega\cos\omega - \cos\Omega\sin\omega\cos i \quad (55)$$

$$Q_{22} = -\sin\Omega\sin\omega - \cos\Omega\cos\omega\cos i \quad (56)$$

$$Q_{23} = -\cos\Omega\sin i \quad (57)$$

$$Q_{31} = \sin\omega\sin i \quad (58)$$

$$Q_{32} = \cos\omega\sin i \quad (59)$$

$$Q_{33} = \cos i, \quad (60)$$

and

$$\boldsymbol{R} = \begin{pmatrix} \cos\nu & \sin\nu & 0 \\ -\sin\nu & \cos\nu & 0 \\ 0 & 0 & 1 \end{pmatrix}. \quad (61)$$

In an attempt to clarify the meaning of Equations (34) and (35), we note here that the latter do not refer to inertial reference frames. The reference frames K_J and K_R are *not inertial* since they are rotating. Equations (34) and (35) constitute a decomposition of the perturbing force into its components in the relevant reference frames and are true at any instant of time. The matrices (51) and (61) are time-dependent since the orbital elements are time-dependent. Thus, the transformations (48)–(50) between the different reference frame components of the force are true at any instant of time. These transformations are constructed in such a way that they include the time derivative of the base unit vectors in K_J and K_R due to the various precessions ($\dot{\omega}$, $\dot{\Omega}$, $\dot{\nu}$). Consequently, the various inertial forces that appear when we transform into a rotating reference frame, namely, K_J and K_R, are already embedded in the form of the *time-dependent rotation matrices* (51) and (61). Inertial forces like Coriolis acceleration, centripetal acceleration, and the Euler acceleration will appear by applying the relevant time-dependent rotation matrix to the position and force vectors and substitute the transformed position and force vectors into the form of the equation of motion in the inertial system. It is after this substitution that the inertial forces appear in their known form.

We note here that Veras et al. (2013) presented Equations (36) and (37) as well as (44) and (45) and were the first to apply them to the study of anisotropic wind mass loss (see Section 5 here and Section 5 in Paper II). However, when choosing the reference system K_J, they incorrectly used in their Equations (35)–(39) the components of the perturbation along the inertial Cartesian system K_I instead of the components of the perturbation in the reference system K_J (compare to our Equations (44) and (45)). As previously mentioned, this is important because the incorrect use of the right set of time evolution equations of the orbital elements for the chosen reference system can lead to a misinterpretation of the evolution changes in the semimajor axis a and eccentricity e.

As we mentioned before, in this paper we are only interested in the time evolution of the semimajor axis and the eccentricity. The basic reason for this is the type of perturbations induced by mass loss/transfer processes. To explain this in more detail, we choose to decompose Equations (18)–(23) in the reference frame K_R:

$$\frac{da}{dt} = \frac{2}{n\sqrt{1-e^2}}[F_r e\sin\nu + F_\tau(1+e\cos\nu)] \quad (62)$$

$$\frac{de}{dt} = \frac{\sqrt{1-e^2}}{na}\left[F_r\sin\nu + F_\tau\left(\cos\nu + \frac{e+\cos\nu}{1+e\cos\nu}\right)\right] \quad (63)$$

$$\frac{di}{dt} = F_n\frac{\cos(f+\omega)\sqrt{1-e^2}}{na(1+e\cos f)} \quad (64)$$

$$\frac{d\Omega}{dt} = \frac{1}{na^2\sqrt{1-e^2}\sin i}F_n\frac{a(1-e^2)\sin(\nu+\omega)}{1+e\cos\nu} \quad (65)$$

$$\frac{d\omega}{dt} = \frac{\sqrt{1-e^2}}{nae}\left(-F_r\cos\nu + F_\tau\sin\nu\frac{2+e\cos\nu}{1+e\cos\nu}\right) - \frac{\cos i}{na\sin i}F_n\frac{\sqrt{1-e^2}\sin(\nu+\omega)}{1+e\cos\nu} \quad (66)$$

$$\frac{d\nu}{dt} = \frac{n(1+e\cos f)^2}{(1-e^2)^{3/2}} - \frac{d\omega}{dt} - \cos i\frac{d\Omega}{dt}. \quad (67)$$

As we will see in the following sections, the perturbations induced by the mass loss/transfer processes studied in this paper have the general form $\boldsymbol{F} \propto \alpha(\nu)\boldsymbol{r} + \beta(\nu)\dot{\boldsymbol{r}}$. From Equations (64) and (65), we can see that the inclination i and the longitude of the ascending node Ω evolve only for a non-zero vertical to the orbital plane component of the perturbing force, i.e., $F_n \neq 0$. However, perturbations of the form $\boldsymbol{F} \propto \alpha(\nu)\boldsymbol{r} + \beta(\nu)\dot{\boldsymbol{r}}$ do not contain such a vertical perturbing force component (i.e., $F_n = 0$), and thus i and Ω do not evolve in the cases we study here. On the contrary, from Equation (66), we see that the argument of periapsis ω is indeed precessing due to mass loss/transfer, but we assume that this precession is small at first-order approximation (i.e., $\dot{\omega} \ll 1$). Under these considerations, we choose to focus on and present only the time evolution of the semimajor axis a and the eccentricity e.

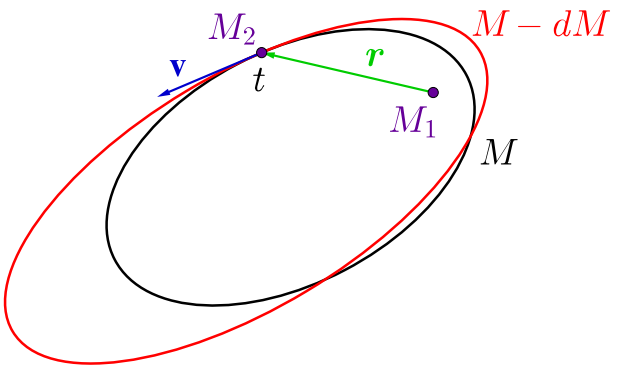

Figure 4. Perturbation induced by instantaneous mass loss dM at time t. The black ellipse is the orbit the body M_2 would follow if there is no total mass change in the system. The red ellipse is the osculating orbit the body would follow if there is a total mass change dM in the system and the perturbation ceased instantaneously. If there is a mass loss at time t, then the velocity $\boldsymbol{v}$ is more than what is needed for the body to follow the black orbit. The linear drag $-\dot{M}/M\dot{\boldsymbol{r}}$ induced forces the body M_2 to follow the osculating red orbit instead.

4. ISOTROPIC WIND MASS LOSS

The components of a binary system can lose mass in many different ways. Due to the energy and angular momentum conservation laws, mass loss procedures expose the system to additional perturbations including linear and angular momentum recoils. One characteristic way through which stars can lose mass is stellar winds. However, the actual form and structure of these winds is a complicated phenomenon and depends strongly on the structure and rotation of the star as well as on the potential existence of a dynamically important magnetic field in the star. In many cases, e.g., in a supernova explosion, the mass loss can be assumed to be spherically symmetric. This means that the wind velocity is the same for all points along the surface of the star, and thus we refer to this case of wind mass loss as *isotropic*. We note here that isotropic mass loss does not produce any momentum kick on the mass-losing body. However, the total mass of the system changes with time, which induces in the system a perturbation which acts as a linear drag force, as we will see below.

As mentioned above, in the case of *isotropic* wind mass loss, the perturbation $\boldsymbol{F}$ in Equation (4) comes implicitly from the fact that the mass of one or both stars is changing, leading to a time-dependent total mass of the system. Figure 4 describes schematically the case of isotropic mass loss considered in this section. Let us assume that at some point t in time, the two-body system has a total mass M and the body M_2 has exactly the needed velocity $\boldsymbol{v}$ to follow the unperturbed orbit (black ellipse in Figure 4). If the total mass of the system momentarily changes by dM introducing no additional momentum kicks to the bodies (what we refer to as isotropic), then the period increases and the velocity $\boldsymbol{v}$ is more than what is needed to follow the unperturbed orbit. The body M_2 will follow the perturbed orbit instead (red ellipse in Figure 4). As we will see below, we can describe this perturbation as a linear drag force acting on the body M_2, forcing it to follow the osculating orbit. Before deriving the actual form of the perturbation, we remind the reader here that the perturbed orbit is an osculating orbit. This means that the body M_2 will never follow the osculating orbit since after time t the total mass of the system will continue changing and the actual physical orbit of the body will never be a closed orbit in time. From Equations (18)–(23), we know that because of the perturbation induced, the osculating orbit will be both evolved and precessed relative to the unperturbed orbit. In Paper II, we will prove that the osculating orbit as already indicated in Figure 4 has on average the same eccentricity, a greater semimajor axis, and precesses compared to the perturbed orbit.

4.1. Perturbing Force Treatment

Hadjidemetriou (1963) and Omarov (1964) independently derived the appropriate perturbation for isotropic wind mass loss. For a donor of mass $M_1(t)$ and a companion of mass $M_2(t)$, if the total mass $M(t) = M_1(t) + M_2(t)$ of the two-body system is changing in time with a rate $\dot{M}(t) < 0$, then making use of the energy equation leads to the following perturbation for isotropic wind mass loss (Hadjidemetriou 1963; Omarov 1964):

$$\boldsymbol{F} = -\frac{1}{2}\frac{\dot{M}(t)}{M(t)}\dot{\boldsymbol{r}}. \tag{68}$$

Perturbation (68) has the form of a linear drag acceleration acting always in the opposite direction to the motion of the body. This linear drag is proportional to the fractional mass loss rate and is responsible for the reduction of the instantaneous velocity magnitude described above and depicted in Figure 4. This reduction leads to the new osculating orbit, which will continue to evolve in time as long as the total mass is continuously changing in time or will be the actual physical orbit of the body if the perturbation ceases instantaneously.

Using the perturbing force (68), the equation of motion (4) becomes

$$\ddot{\boldsymbol{r}} = -\frac{GM}{r^3}\boldsymbol{r} - \frac{1}{2}\frac{\dot{M}(t)}{M(t)}\dot{\boldsymbol{r}}. \tag{69}$$

For the perturbation defined by Equation (68), making use of relations (125)–(145) in Equations (18) and (19), one derives the following phase-dependent time evolution equations for the osculating semimajor axis and eccentricity in the case of isotropic wind mass loss (Hadjidemetriou 1963)

$$\left(\frac{da}{dt}\right)_{\rm iso} = -\frac{(1 + e^2 + 2e\cos\nu)}{1 - e^2}\frac{\dot{M}}{M}a \tag{70}$$

$$\left(\frac{de}{dt}\right)_{\rm iso} = -(e + \cos\nu)\frac{\dot{M}}{M}. \tag{71}$$

Equations (70) and (71) show that the osculating semimajor axis and eccentricity are generally phase-dependent. Using the identity $\cos^2\nu + \sin^2\nu = 1$, we can re-write the nominator in Equation (70) as $(e + \cos\nu)^2 + \sin^2\nu$, which is always positive. This proves that for any isotropic mass loss, the semimajor axis can never decrease throughout the orbit and is not oscillating. Following the same procedure, and given that the periastron position is given by $r_p = a(1 - e)$, one can prove that $\dot{r}_p = -\frac{(1-e)(1-\cos\nu)}{1+e}\frac{\dot{M}}{M}a$. Since $e < 1$ and $\cos\nu < 1$ always for any isotropic mass loss, the periastron position can never decrease throughout the orbit and also is not oscillating. However, the eccentricity does not follow a similar behavior and can both increase and decrease throughout the orbit. The eccentricity undergoes oscillations on an orbital timescale (see e.g., Veras et al. 2011). The amplitude of these oscillations is

proportional to $\dot{M}/nM$, which is a scaled ratio of the orbital period to the mass loss timescale. These oscillations can be smoothed out through orbit-averaging procedures when deriving the secular time evolution equations of the osculating orbital elements. These secular time evolution equations can be even more simplified in the adiabatic regime (see Section 2.1.2 and Paper II for more details). Over time, the amplitude of these oscillations is increasing, since eventually the orbital period increases and becomes comparable to the mass loss timescale. This is the point where adiabaticity is broken and the "adiabatic" equations no longer apply.

4.2. Perturbing Lagrangian Treatment

Equations (70) and (71) can alternatively be derived from Equations (26) and (27) for a zero-gauge ($\boldsymbol{\Phi} = 0$) by applying the perturbing Lagrangian

$$\Delta L = f(M_1, M_2)\left(\frac{1}{2}\dot{\boldsymbol{r}}^2 + \frac{GM}{r}\right), \tag{72}$$

where $f(M_1, M_2) = \frac{1}{2}\ln\frac{M}{M_0}$, with M_0 being a constant equal to the the total mass of the system at $t = 0$.

We note here that the Lagrangian (72) was derived in such a way that it satisfies Equation (25) with the force given by Equation (68). Since Equation (25) cannot uniquely determine the relative Lagrangian for a given force, the Lagrangian (72) is not unique, has no physical meaning, and it acts mainly as a mathematical tool to derive the time evolution of the osculating or non-osculating orbital elements through Equations (26) and (27), also allowing for the gauge freedom. This freedom in the choice of the Lagrangian is depicted in the freedom in the functional dependence of the function f on M_1 and M_2. This means that the osculating orbital elements which have a specific physical interpretation cannot depend on the function f and one can prove that Equations (26) and (27) are constructed in such a way that for a zero-gauge that leads to the osculating orbital elements, the functional dependence on f diminishes. However, for a non-zero-gauge, and thus non-osculating orbital elements with no physical meaning, this is no longer true. For the generalized Lagrange constraint given in Equation (32) and isotropic wind mass loss, the phase-dependent time evolution equations for the contact orbital elements (see Section 2.1.2) are given by

$$\left(\frac{da_{\rm con}}{dt}\right)_{\rm iso} = \frac{f(f+2)}{f+1}\left[\frac{-2nae\sin\nu(1+e\cos\nu)^2}{(1-e^2)^{5/2}}\right] \tag{73}$$

$$\left(\frac{de_{\rm con}}{dt}\right)_{\rm iso} = \frac{f(f+2)}{f+1}\left[\frac{-n\sin\nu(1+e\cos\nu)^2}{(1-e^2)^{3/2}}\right]. \tag{74}$$

We note here that Equations (73) and (74) depend on the arbitrary function f because they describe the time evolution of the so-called contact elements which, as we mentioned before, do not have physical meaning. In the case of the non-zero-gauge (32), both the contact semimajor axis and the eccentricity oscillate throughout the orbit. In Paper II, we compare the orbit-averaged time evolution equations for the osculating and contact orbital elements assuming either adiabaticity or delta-function mass loss at periastron.

5. ANISOTROPIC WIND MASS LOSS

Stellar mass loss is time-dependent and depends generally on the latitude and longitude along the surface of the star. For example, there is significant observational evidence that the equatorial regions around rapidly rotating hot stars generally have an enhanced wind density, perhaps even (e.g., as in Be stars) a circumstellar disk (e.g., Owocki et al. 1998). More recent studies assume that the Be-star wind has a disk component in the equatorial plane plus a weak spherical wind above the poles (e.g., Bogomazov 2005).

The formation of bipolar jets is strongly linked with accretion onto protostars. Since the accretion process can persist for a long time after the star is born, jets usually accompany a disk (e.g., Blandford & Payne 1982)

In this section, we do not study the case of a circumstellar disk. However, we assume that the mass-flux rate as well as the wind velocity is different at each point along the spherical surface of the star. Here, we refer to this case as *anisotropic* wind mass loss. The results of this section are also applicable to the case of anisotropic planet evaporation (including jets) around the host star in a planet-star binary system (e.g., Boué et al. 2012; Veras et al. 2013).

Veras et al. (2013) were the first to study the case of anisotropic wind mass loss from the star in a star-planet binary system. However, as we mentioned in Section 3, in this work, there are some inconsistencies arising from a mistreated transformation from one reference system to the other. Both the importance of the choice of reference frame and the importance of the use of the right set of equations for the reference system chosen were also pointed out in Section 3. For the case of anisotropic wind mass loss that we describe here, we discuss in Paper II the effect of the corrected time evolution equations we derived in Section 3 (see Equations (44) and (45)) on the secular time evolution equations of the orbital elements.

If the mass-losing body of mass $M_1(t)$ has a mass loss flux per solid angle $J(\phi, \theta, t) > 0$, then we can express the mass loss rate $\dot{M}_1$ as

$$\dot{M}_1 = -\frac{1}{4\pi}\int_0^{\pi}\int_0^{2\pi} J(\phi, \theta, t)\sin\theta d\phi d\theta, \tag{75}$$

where ϕ and θ are the longitude and co-latitude, respectively, on the surface of the mass-losing body (donor).

If the mass at a specific point is lost with a velocity of $\boldsymbol{u}(\phi, \theta, t)$ relative to the center-of-mass and along the radius of the donor, then assuming the spin axis of the donor to be fixed with respect to the orbit, the perturbing acceleration $\boldsymbol{A}_{\rm aniso}$ arising from the anisotropic wind mass loss is given by

$$\boldsymbol{A}_{\rm aniso} = -\frac{\boldsymbol{F}_{\rm aniso}}{M_1(t)}, \tag{76}$$

where $\boldsymbol{F}_{\rm aniso}$ is the perturbing force arising from the anisotropic wind mass loss. In the inertial reference system $K_I(\hat{\boldsymbol{x}}, \hat{\boldsymbol{y}}, \hat{\boldsymbol{z}})$ mentioned in Section 3 and depicted in Figure 3, the components of this perturbing force are given by

$$F_{{\rm aniso},x} = \frac{1}{4\pi}\int_0^{\pi}\int_0^{2\pi} J(\phi, \theta, t)u(\phi, \theta, t)d\phi\sin\theta\cos\phi d\theta \tag{77}$$

$$F_{\mathrm{aniso},y} = \frac{1}{4\pi}\int_0^{\pi}\int_0^{2\pi} J(\phi,\,\theta,\,t)u(\phi,\,\theta,\,t)d\phi\,\sin\theta\,\sin\phi d\theta \tag{78}$$

$$F_{\mathrm{aniso},z} = \frac{1}{4\pi}\int_0^{\pi}\int_0^{2\pi} J(\phi,\,\theta,\,t)u(\phi,\,\theta,\,t)d\phi\,\cos\theta d\theta. \tag{79}$$

It is important to mention here that neither the velocity $u(\phi,\,\theta,\,t)$ nor the mass-flux rate $J(\phi,\,\theta,\,t)$ depend on the relative position between the two bodies in the binary system. Thus, based on Equations (76)–(79), one can see that the perturbing force $\boldsymbol{F}_{\mathrm{aniso}}$ is not phase-dependent. However, both the mass loss rate and the mass of the donor, and thus both the perturbing force and acceleration, remain time-dependent. In a manner similar to the isotropic wind mass loss case (see Section 4) where the mass loss rate and the total mass was a function of time, this time dependence induces implicitly a perturbation, even though this perturbation is not explicitly phase-dependent. In Paper II, we derive the secular time evolution equations for the osculating orbital elements in the case of anisotropic wind mass loss and for the phase-independent perturbing acceleration described by Equations (76)–(79).

Picking a different reference system can lead to equations that are more easy to qualitatively interpret. Given the fact that the wind structure depends on the rotation of the star as well as its magnetic field, we usually describe the form of the wind in the inertial reference frame K_I. However, given the form of the wind in this system, we can calculate the inertial perturbing force components and we can then transform for considerable simplifications to the reference system K_J using Equation (48) or to reference system K_R using Equation (49). In these new systems, the perturbing force components are given, respectively, by

$$\begin{pmatrix} F_{\mathrm{aniso},p} \\ F_{\mathrm{aniso},q} \\ F_{\mathrm{aniso},l} \end{pmatrix} = \begin{pmatrix} Q_{11} & Q_{21} & Q_{31} \\ Q_{12} & Q_{22} & Q_{32} \\ Q_{13} & Q_{23} & Q_{33} \end{pmatrix} \begin{pmatrix} F_{\mathrm{aniso},x} \\ F_{\mathrm{aniso},y} \\ F_{\mathrm{aniso},z} \end{pmatrix} \tag{80}$$

and

$$\begin{pmatrix} F_{\mathrm{aniso},r} \\ F_{\mathrm{aniso},\tau} \\ F_{\mathrm{aniso},n} \end{pmatrix} = \begin{pmatrix} \cos\nu & \sin\nu & 0 \\ -\sin\nu & \cos\nu & 0 \\ 0 & 0 & 1 \end{pmatrix} \begin{pmatrix} F_{\mathrm{aniso},p} \\ F_{\mathrm{aniso},q} \\ F_{\mathrm{aniso},l} \end{pmatrix}. \tag{81}$$

In Paper II, we examine qualitatively some simple structures of anisotropic wind mass loss including jets. We initially begin by describing the wind structure in the inertial reference frame $K_I(\hat{\boldsymbol{x}}, \hat{\boldsymbol{y}}, \hat{\boldsymbol{z}})$ and then, by transforming to different reference systems that simplify our Equations (reference systems K_R and K_J), we derive the secular time evolution equations of the orbital elements in these systems in the adiabatic regime.

6. NON-ISOTROPIC EJECTION/ACCRETION IN MASS TRANSFER (REACTION FORCES)

Wind mass loss is only one of the ways two bodies in a binary system can exchange mass. Another possibility is mass ejection or accretion from specific points and with specific velocities. Due to linear momentum conservation, this ejection and accretion induces kicks/reaction forces to the mass-losing and the mass-accreting star, respectively. To distinguish this mass transfer process from the case of anisotropic wind mass loss, we choose to refer to this process as *non-isotropic* ejection/accretion.

The most characteristic example of anisotropic ejection/accretion is RLOF. In this case, the mass is ejected from the Lagrangian point L_1. This mass can (i) escape from the system, (ii) be re-accreted from the donor (self-accretion), (iii) hit the radius of the accretor (direct impact), or (iv) hit the radius of an accretion disk that has been formed around the companion (e.g., Sepinsky et al. 2007, 2009, 2010). We refer to the case when all of the mass ejected is accreted as conservative mass transfer while the case when some mass is lost from the system is referred to as non-conservative.

In the next two sections, we study the cases of non-isotropic ejection and accretion in both a conservative and non-conservative manner, keeping the ejection/accretion points and velocities as general parameters of the problem.

6.1. Conservative Case ($\dot{M} = \dot{J}_{\mathrm{orb}} = 0$)

We assume an eccentric binary system consisting of two masses $M_1(t)$ and $M_2(t)$. We refer to these bodies as the donor and the accretor, respectively.

Binary component #1 loses mass at a rate of $\dot{M}_1 < 0$, with absolute velocity $\boldsymbol{w}_1$ and from point $\boldsymbol{r}_{A_1}$ relative to the center-of-mass of the body. Binary component #2 accretes mass at a rate of $\dot{M}_2 > 0$, with absolute velocity $\boldsymbol{w}_2$ and to point $\boldsymbol{r}_{A_2}$ relative to the center-of-mass of the body. The mass transfer stream is assumed to remain always confined to the orbital plane.

Following the work of Hadjidemetriou (1963) and Sepinsky et al. (2007), the equation of motion of the two-body system can be written in an inertial frame as follows:

$$\begin{aligned}\ddot{\boldsymbol{r}} = &-\frac{G(M_1+M_2)}{r^3}\boldsymbol{r} + \frac{\dot{M}_2}{M_2}(\boldsymbol{w}_2 + \boldsymbol{\omega}_{\mathrm{orb}}\times\boldsymbol{r}_{A_2}) \\ &- \frac{\dot{M}_1}{M_1}(\boldsymbol{w}_1 + \boldsymbol{\omega}_{\mathrm{orb}}\times\boldsymbol{r}_{A_1}) - \frac{\dot{M}_2}{M_2}\boldsymbol{v}_2 + \frac{\dot{M}_1}{M_1}\boldsymbol{v}_1 \\ &+ \frac{\ddot{M}_2}{M_2}\boldsymbol{r}_{A_2} - \frac{\ddot{M}_1}{M_1}\boldsymbol{r}_{A_1}\end{aligned} \tag{82}$$

$$\begin{aligned}= &-\frac{G(M_1+M_2)}{r^3}\boldsymbol{r} + \frac{\dot{M}_2}{M_2}(\boldsymbol{w}_2 - \boldsymbol{v}_2 + \boldsymbol{\omega}_{\mathrm{orb}}\times\boldsymbol{r}_{A_2}) \\ &- \frac{\dot{M}_1}{M_1}(\boldsymbol{w}_1 - \boldsymbol{v}_1 + \boldsymbol{\omega}_{\mathrm{orb}}\times\boldsymbol{r}_{A_1}) \\ &+ \frac{\ddot{M}_2}{M_2}\boldsymbol{r}_{A_2} - \frac{\ddot{M}_1}{M_1}\boldsymbol{r}_{A_1}\end{aligned} \tag{83}$$

where $\boldsymbol{v}_1$ and $\boldsymbol{v}_2$ are the orbital velocities of the two bodies with respect to the inertial frame and $\boldsymbol{\omega}_{\mathrm{orb}}$ is the orbital angular frequency. Equation (83) takes into account the motion of the center-of-mass of the bodies and ignores the forces on the bodies from the mass transfer stream under the assumption that the stream's mass is negligible. We note here that when writing the linear momentum conservation equations, we assume the absolute velocities $\boldsymbol{w}_1$ and $\boldsymbol{w}_2$ to be in the direction opposite to the direction of motion of the bodies.

From Equation (83), we can see that anisotropic accretion and ejection introduces the reaction forces

$$\frac{\dot{M}_2}{M_2}(\boldsymbol{w}_2 - \boldsymbol{v}_2 + \boldsymbol{\omega}_{\mathrm{orb}}\times\boldsymbol{r}_{A_2}) \tag{84}$$

$$-\frac{\dot{M}_1}{M_1}(\boldsymbol{w}_1 - \boldsymbol{v}_1 + \boldsymbol{\omega}_{\rm orb} \times \boldsymbol{r}_{A_1}), \tag{85}$$

for accretion and ejection, respectively. The terms with the second-order time derivative in Equation (83) are related to the acceleration of the centers-of-mass of the two stars relative to their positions in the unperturbed no mass loss case (see Section 2 in Sepinsky et al. 2007 for a detailed description of the relevant terms).

The reaction forces (84) and (85) emerge from applying the linear momentum conservation law in the accretor and the donor, respectively. As a reminder, we mention here that in the isotropic mass ejection/accretion case, we have

$$\sum_i \{(\boldsymbol{w}_1 - \boldsymbol{v}_1)_i + \boldsymbol{\omega}_{\rm orb} \times \boldsymbol{r}_{A_{1i}}\} = 0 \tag{86}$$

$$\sum_i \{(\boldsymbol{w}_2 - \boldsymbol{v}_2)_i + \boldsymbol{\omega}_{\rm orb} \times \boldsymbol{r}_{A_{2i}}\} = 0. \tag{87}$$

These terms are zero due to isotropy.

If all of the mass lost from the donor is accreted by the companion, and any orbital angular momentum transported by the transferred mass is immediately returned to the orbit, then, as we mentioned before, the mass transfer is conservative. In this case, both the total system mass and orbital angular momentum are conserved and we can then write $\dot{M}_2 = -\dot{M}_1$, $\ddot{M}_2 = -\ddot{M}_1$. Equations (82) and (83) in the case of conservative mass transfer yield

$$\begin{aligned}\ddot{\boldsymbol{r}} =& -\frac{G(M_1+M_2)}{r^3}\boldsymbol{r} \\ &+ \dot{M}_2\left(\frac{\boldsymbol{w}_2}{M_2} + \frac{\boldsymbol{\omega}_{\rm orb}\times\boldsymbol{r}_{A_2}}{M_2} + \frac{\boldsymbol{w}_1}{M_1} + \frac{\boldsymbol{\omega}_{\rm orb}\times\boldsymbol{r}_{A_1}}{M_1}\right) \\ &+ \ddot{M}_2\left(\frac{\boldsymbol{r}_{A_2}}{M_2} + \frac{\boldsymbol{r}_{A_1}}{M_1}\right) - \dot{M}_2\left(\frac{\boldsymbol{v}_1}{M_1} + \frac{\boldsymbol{v}_2}{M_2}\right) \qquad (88)\\ =& -\frac{G(M_1+M_2)}{r^3}\boldsymbol{r} + \boldsymbol{b} - \dot{M}_2\left(\frac{\boldsymbol{v}_1}{M_1} + \frac{\boldsymbol{v}_2}{M_2}\right), \qquad (89)\end{aligned}$$

where for convenience we set

$$\begin{aligned}\boldsymbol{b} \equiv& \dot{M}_2\left(\frac{\boldsymbol{w}_2}{M_2} + \frac{\boldsymbol{\omega}_{\rm orb}\times\boldsymbol{r}_{A_2}}{M_2} + \frac{\boldsymbol{w}_1}{M_1} + \frac{\boldsymbol{\omega}_{\rm orb}\times\boldsymbol{r}_{A_1}}{M_1}\right) \\ &+ \ddot{M}_2\left(\frac{\boldsymbol{r}_{A_2}}{M_2} + \frac{\boldsymbol{r}_{A_1}}{M_1}\right). \qquad (90)\end{aligned}$$

Taking into account the center-of-mass of the two bodies' motion, we can write the positions of the donor and the accretor as

$$\boldsymbol{r}_1 = \boldsymbol{r}_{\rm cm} - \frac{M_2}{M_1+M_2}\boldsymbol{r} \tag{91}$$

$$\boldsymbol{r}_2 = \boldsymbol{r}_{\rm cm} + \frac{M_1}{M_1+M_2}\boldsymbol{r}. \tag{92}$$

The time derivative of Expressions (91) and (92) then gives

$$\frac{\boldsymbol{v}_1}{M_1} = \frac{\boldsymbol{v}_{\rm cm}}{M_1} - \frac{\dot{M}_2}{MM_1}\boldsymbol{r} - \frac{M_2}{M_1 M}\dot{\boldsymbol{r}} \tag{93}$$

$$\frac{\boldsymbol{v}_2}{M_2} = \frac{\boldsymbol{v}_{\rm cm}}{M_2} + \frac{\dot{M}_1}{MM_2}\boldsymbol{r} - \frac{M_1}{M_2 M}\dot{\boldsymbol{r}}. \tag{94}$$

In the conservative case, we have $\dot{M}_2 = -\dot{M}_1$, and at first order the last term in the right-hand side (RHS) of Equation (89) becomes

$$-\dot{M}_2\left(\frac{\boldsymbol{v}_1}{M_1} + \frac{\boldsymbol{v}_2}{M_2}\right) = -\dot{M}_2\left(\frac{1}{M_2} - \frac{1}{M_1}\right)\dot{\boldsymbol{r}} \tag{95}$$

so that the perturbing force in this case can be re-written as

$$\begin{aligned}\boldsymbol{F} &= \boldsymbol{b} - \dot{M}_2\left(\frac{1}{M_2} - \frac{1}{M_1}\right)\dot{\boldsymbol{r}} \qquad (96)\\ &= \boldsymbol{b} - h\dot{\boldsymbol{r}}, \qquad (97)\end{aligned}$$

where we defined

$$h \equiv \dot{M}_2\left(\frac{1}{M_2} - \frac{1}{M_1}\right). \tag{98}$$

Applying Equations (18) and (19) with a perturbing force of the form (97), also using Equations (90) and (98), gives the following phase-dependent time evolution equations for the semimajor axis and eccentricity in the conservative mass transfer case:

$$\begin{aligned}\left(\frac{da}{dt}\right)_{\rm con} =& \frac{2}{n\sqrt{1-e^2}}[b_r e\sin\nu + b_\tau(1+e\cos\nu)] \\ &- 2ha\left[\frac{e^2+2e\cos\nu+1}{1-e^2}\right] \qquad (99)\\ \left(\frac{de}{dt}\right)_{\rm con} =& \frac{(1-e^2)^{1/2}}{na}[b_r\sin\nu \\ &+ b_\tau\frac{2\cos\nu + e(1+\cos^2\nu)}{1+e\cos\nu}] \\ &- 2h[e+\cos\nu], \qquad (100)\end{aligned}$$

where b_r and b_τ are the radial and tangential components of the quantity $\boldsymbol{b}$ defined in Equation (90) and depend on the set up of each problem under consideration. We note here that the quantity $\boldsymbol{b}$ does not depend on the relative position between the two bodies in the binary, i.e., it is phase-independent. This is something useful to keep in mind when we perform orbit-averaging processes on Equations (99) and (100). In Paper II, we derive the secular time evolution equations of the orbital elements for the conservative mass transfer case in both the adiabatic regime as well as under the assumption of a delta-function mass loss/transfer at periastron.

If one wants to introduce a different gauge, then the same equations can be derived from Equations (26) and (27) using the Lagrangian

$$\Delta L = \boldsymbol{b}\boldsymbol{r} + f(M_1, M_2)\left(\frac{1}{2}\dot{\boldsymbol{r}}^2 + \frac{GM}{r}\right), \tag{101}$$

where $f(M_1, M_2) = \log\left(\frac{M_2}{M_1}\right) - 2\log\left(1+\frac{M_2}{M_1}\right)$.

It is important to mention that the functional form of $f(M_1, M_2)$ does not affect the final evolution equations for the osculating orbital elements, which have a physical meaning in the problem. Equations (26) and (27) are constructed in such a way that the terms that depend on $f(M_1, M_2)$ cancel each other out. This is expected since the freedom in the choice of the Lagrangian should not affect the final physical result. In this formulation, the Lagrangian does not have a clear physical

interpretation on its own and acts more like a mathematical tool. However, it remains useful when one wants to explore the gauge freedom in orbital mechanics. If one uses the Lagrangian (101) for *non-osculating* orbital elements that have no physical meaning, then there is a dependence on $f(M_1, M_2)$ in the final equations, as we can easily see using the generalized Lagrange constraint defined by Equation (32). Since in this gauge

$$\boldsymbol{\Phi} + \frac{\partial \Delta L}{\partial \dot{\boldsymbol{r}}} = 0, \tag{102}$$

Equations (26) and (27) for the so-called *contact* orbital elements simplify to

$$\frac{da_{\rm con}}{dt} = \frac{2}{na}\left[\frac{\partial(-\Delta H^c)}{\partial \sigma}\right] \tag{103}$$

$$\frac{de_{\rm con}}{dt} = \frac{1-e^2}{na^2 e}\left[\frac{\partial(-\Delta H^c)}{\partial \sigma}\right] - \frac{\sqrt{1-e^2}}{na^2 e}\left[\frac{\partial(-\Delta H^c)}{\partial \omega}\right], \tag{104}$$

where we defined the non-osculating perturbing Hamiltonian as ΔH^c. This Hamiltonian has a different functional dependence on $(\boldsymbol{r}, \dot{\boldsymbol{r}})$ from the relative $\Delta H^{\rm osc}$ computed in the case of osculating orbital elements using a zero-gauge $\boldsymbol{\Phi} = 0$.

Using the perturbing Lagrangian (101) and applying the gauge (32) into Equations (103) and (104), we have the following phase-dependent time evolution equations for the so-called *contact* orbital elements:

$$\left(\frac{da_{\rm con}}{dt}\right)_{\rm con} = \frac{2}{n\sqrt{1-e^2}}[b_r e \sin\nu + b_\tau(1+e\cos\nu)] - \frac{2nae\sin\nu(1+e\cos\nu)^2}{(1-e^2)^{5/2}}\left[\frac{f(f+2)}{f+1}\right] \tag{105}$$

$$\left(\frac{de_{\rm con}}{dt}\right)_{\rm con} = \frac{(1-e^2)^{1/2}}{na}[b_r \sin\nu + b_\tau \frac{2\cos\nu + e(1+\cos^2\nu)}{1+e\cos\nu}] - \frac{n\sin\nu(1+e\cos\nu)^2}{(1-e^2)^{3/2}}\left[\frac{f(f+2)}{f+1}\right]. \tag{106}$$

As we noted previously, Equations (105) and (106) depend on the functional form of the arbitrary function f, and thus cannot be attributed any physical meaning. However, as we mentioned in previous sections, in some cases, time evolution equations of non-osculating elements can prove useful and are presented here for completeness. In Paper II, we derive and compare the relative secular time evolution equations for the osculating and contact orbital elements, respectively, under the assumption of adiabaticity.

6.2. Non-conservative Case, $\dot{M}, \dot{J}_{\rm orb} \neq 0$

In most astrophysical binaries, only a fraction γ of the ejected mass is accreted by the companion, i.e., $\dot{M}_2 = -\gamma \dot{M}_1$, $\dot{M} = (1-\gamma)\dot{M}_1$. The rest of the mass is lost from the system carrying along with it some fraction $\zeta > 0$ of the total orbital angular momentum. In this case of non-conservative mass transfer, one should also include the perturbations arising from the loss of total mass and orbital angular momentum.

The total angular momentum of the system can change because of three reasons: (i) the velocities of the donor and the accretor change due to mass ejection and accretion, respectively, (ii) the total system mass changes, and (iii) the lost mass carries away an excess amount of orbital angular momentum that is not implicitly hidden in the mass and velocity change.

We have considered the perturbation arising from case (i) in the previous section of conservative mass transfer. The additional perturbation from cases (ii) and (iii) is described by

$$-\frac{1}{2}(\zeta+1)\frac{\dot{M}}{M}\dot{\boldsymbol{r}}, \tag{107}$$

where the extra angular momentum carried away by the mass lost from the system is parameterized in terms of the specific angular momentum of the orbit using the parameter ζ defined as follows:

$$\frac{\dot{J}_{\rm orb}}{J_{\rm orb}} = \zeta\frac{\dot{M}}{M}. \tag{108}$$

The parameter ζ is a function of time (phase-dependent) depending in principle on both the orbital elements and the stellar properties of the binary components (see the second and third paragraphs from the end in the current section for details).

The first term in the parentheses refers to the perturbation from case (iii), expressing the carried-away angular momentum as a fraction of the total orbital angular momentum. The second term refers to the perturbation from case (ii), where we have assumed similar arguments as those described for the case of isotropic wind mass loss in Section 4 and depicted in Figure 4 (compare also Equation (68) in Section 4). We note here that the form of perturbation will vary if other assumptions about the mass loss characteristics are made.

The total perturbation will then be given by

$$\boldsymbol{F}_{\text{non-con}} = \boldsymbol{F}_{\rm con} - \frac{1}{2}(\zeta+1)\frac{\dot{M}}{M}\dot{\boldsymbol{r}} \Rightarrow \tag{109}$$

$$\boldsymbol{F}_{\text{non-con}} = \boldsymbol{b} - h\dot{\boldsymbol{r}} - \frac{1}{2}(\zeta+1)\frac{\dot{M}}{M}\dot{\boldsymbol{r}}, \tag{110}$$

where the conservative mass transfer perturbing force is given as described in the previous section by

$$\boldsymbol{F}_{\rm con} = +\frac{\dot{M}_2}{M_2}(\boldsymbol{w}_2 - \boldsymbol{v}_2 + \boldsymbol{\omega}_{\rm orb}\times\boldsymbol{r}_{A_2}) - \frac{\dot{M}_1}{M_1}(\boldsymbol{w}_1 - \boldsymbol{v}_1 + \boldsymbol{\omega}_{\rm orb}\times\boldsymbol{r}_{A_1}) + \frac{\ddot{M}_2}{M_2}\boldsymbol{r}_{A_2} - \frac{\ddot{M}_1}{M_1}\boldsymbol{r}_{A_1} \tag{111}$$

, and $\boldsymbol{b}$ and h are defined in the non-conservative case by

$$\boldsymbol{b} \equiv \dot{M}_2\left(\frac{\boldsymbol{w}_2}{M_2} + \frac{\boldsymbol{\omega}_{\rm orb}\times\boldsymbol{r}_{A_2}}{M_2} + \frac{\boldsymbol{w}_1}{M_1} + \frac{\boldsymbol{\omega}_{\rm orb}\times\boldsymbol{r}_{A_1}}{M_1}\right) + \ddot{M}_2\left(\frac{\boldsymbol{r}_{A_2}}{M_2} + \frac{\boldsymbol{r}_{A_1}}{M_1}\right) \tag{112}$$

$$h \equiv \dot{M}_2\left(\frac{1}{M_2} - \frac{1}{M_1}\right) \tag{113}$$

$$\dot{M}_2 = \dot{M}_{2,\rm acc} = -\gamma \dot{M}_1 \tag{114}$$

$$\dot{M}_1 = -\dot{M}_{2,\rm acc} = \dot{M}_{1,\rm acc} = \gamma \dot{M}_1 \tag{115}$$

$$\dot{M} = (1-\gamma)\dot{M}_1. \tag{116}$$

The general perturbation (110) now leads to the most general phase-dependent time evolution equations for the semimajor axis and eccentricity in the non-conservative mass transfer case:

$$\left(\frac{da}{dt}\right)_{\rm non\text{-}con} = \frac{2}{n\sqrt{1-e^2}}[b_r e \sin\nu + b_\tau(1+e\cos\nu)] - 2ha\left[\frac{e^2+2e\cos\nu+1}{1-e^2}\right] - (\zeta+1)\left[\frac{e^2+2e\cos\nu+1}{1-e^2}\right]\frac{\dot{M}}{M} \tag{117}$$

$$\left(\frac{de}{dt}\right)_{\rm non\text{-}con} = \frac{(1-e^2)^{1/2}}{na}[b_r \sin\nu + b_\tau \frac{2\cos\nu + e(1+\cos^2\nu)}{1+e\cos\nu}] - 2h[e+\cos\nu] - (\zeta+1)[e+\cos\nu]\frac{\dot{M}}{M}. \tag{118}$$

Equations (117) and (118) include all of the effects on the evolution of the semimajor axis and eccentricity from non-isotropic ejection and accretion in the binary system.

The first terms in the RHS of Equations (117) and (118) are related to the absolute velocities of the ejected and accreted matter as well as to the point where the ejection and accretion takes place. This information is hidden in the radial and tangential components of the parameter $\boldsymbol{b}$ defined by Equation (90). We mention here that the knowledge of the final accretion points and velocities given the initial ones requires the full solution of the two-body plus a mass transfer stream problem. Applications have been undertaken to approximate the mass transfer stream as a third point particle and numerically integrate the equations of motion assuming ballistic trajectories (e.g., Sepinsky et al. 2010; Davis et al. 2014).

The second terms in the RHS of Equations (117) and (118) refer to the mass that is accreted. The accreted mass is parametrized with γ defined in Equation (114), while the perturbation has the form of h defined in Equation (113). The fraction of accreted mass γ is a free parameter in a problem but can be constrained using ballistic or hydrodynamic simulations. Furthermore, for phase-dependent mass transfer the accreted mass can also be confined, e.g., following the Bondi–Hoyle accretion scenario. The case of phase-dependent mass transfer will be discussed in detail in Paper II.

The last terms in Equations (117) and (118) refer to the mass lost from the system parametrized by γ as well as the orbital angular momentum this mass carries with it parametrized by ζ. The second term inside the square brackets refers to the former while the first one refers to the latter.

We note here that the ζ-dependent term refers to the additional angular momentum removed by the lost mass, i.e., to the change in the total orbital angular momentum rather than that due to the total system mass change. The sources of this additional angular momentum are many. They include the extra angular momentum that the mass transfer stream gains when moving from the donor to the accretor and exchanges of angular momentum between the orbit and the stellar spins due to tidal torques. Here, we express this amount of angular momentum removal as a part of the total orbital angular momentum. This is strongly dependent on the specific assumptions made in the set up of each problem. For example, if we assume that the total mass lost from the system occurs in the vicinity of the accretor, carrying along with it the specific angular momentum of the latter, then we have $\zeta = M_1/M_2$ (e.g., Soberman et al. 1997; Sepinsky et al. 2009). In general, ζ is a free parameter and its value can be restricted using three-body ballistic trajectories (e.g., Flannery 1975; Brookshaw & Tavani 1993; and Appendix A.3 of de Mink et al. 2013 for a review). Another approach for limiting some of the aforementioned free parameters, incuding mass transfer rates, is to study mass transfer with SPH simulations (e.g., Regös et al. 2005; Church et al. 2009; Lajoie & Sills 2011).

Here, we note that in the limiting case of $\zeta \to 0$ (no extra angular momentum removed from the system), the last terms in the RHS of Equations (117) and (118) become equivalent to the terms in the RHS of Equations (70) and (71) presented in Section 4 in the case of isotropic wind mass loss. This emerges from the fact that when there is no extra angular momentum carried away from the system, the orbital evolution induced by the change in the total orbital momentum is implicitly induced by the total mass change with time. Any extra angular momentum removed from the system is parametrized by $\zeta \neq 0$ and induces an additional orbital evolution of the system, while this effect is maximized in the limiting case of $\zeta \to 1$.

In this section, we presented the form of the phase-dependent time evolution equations of the orbital elements in the most general case of non-conservative mass transfer assuming extended bodies. In Paper II, we orbit-average these equations and derive the secular time evolution equations of the orbital elements for the non-conservative case in the adiabatic regime as well as under delta-function mass loss/transfer at periastron.

7. POINT-MASS APPROXIMATION

The validity of any model describing mass loss and mass transfer in a binary system (e.g., the Roche model) relies on two assumptions: that the stellar components can be treated as point masses and that the donor star is rotating synchronously with the orbit. For the latter approximation, we assume that the bodies are synchronized with the orbit. For the former approximation, here we present the form the perturbing force and the time evolution equations of the orbital elements reduce to in the case of point masses.

Under the point-mass approximation, the positions of the ejection and accretion points relative to the center-of-mass of the bodies is zero, and so we have $\boldsymbol{r}_{A1} = \boldsymbol{r}_{A2} = 0$. Using Equations (109) and (111), the perturbing force in this case is reduced to

$$\boldsymbol{F}_{\rm non\text{-}con} = \frac{\dot{M}_2}{M_2}(\boldsymbol{w}_2 - \boldsymbol{v}_2) - \frac{\dot{M}_1}{M_1}(\boldsymbol{w}_1 - \boldsymbol{v}_1) - \frac{1}{2}(\zeta+1)\frac{\dot{M}}{M}\dot{\boldsymbol{r}} \tag{119}$$

$$= \boldsymbol{c} - k\dot{\boldsymbol{r}}, \tag{120}$$

where we defined

$$\boldsymbol{c} \equiv \frac{\dot{M}_2}{M_2}(\boldsymbol{w}_2 - \boldsymbol{v}_2) - \frac{\dot{M}_1}{M_1}(\boldsymbol{w}_1 - \boldsymbol{v}_1), \tag{121}$$

and

$$k \equiv \frac{1}{2}(\zeta + 1)\frac{\dot{M}}{M}. \tag{122}$$

Making use of Equations (120)–(122), Equations (117) and (118) give the phase-dependent time evolution equations of the semimajor axis and eccentricity for non-conservative mass transfer, and in the case of point masses

$$\left(\frac{da}{dt}\right)^{\text{point}}_{\text{non-con}} = \frac{2}{n\sqrt{1-e^2}}[c_r e \sin\nu + c_\tau(1 + e\cos\nu)] - (\zeta + 1)\left[\frac{e^2 + 2e\cos\nu + 1}{1 - e^2}\right]\frac{\dot{M}}{M} \tag{123}$$

$$\left(\frac{de}{dt}\right)^{\text{point}}_{\text{non-con}} = \frac{(1-e^2)^{1/2}}{na}[c_r \sin\nu + c_\tau \frac{2\cos\nu + e(1 + \cos^2\nu)}{1 + e\cos\nu}] - (\zeta + 1)[e + \cos\nu]\frac{\dot{M}}{M}, \tag{124}$$

where now c_r and c_τ are the radial and tangential components, respectively, of the quantity $\boldsymbol{c}$ defined in Equation (121). These components depend only on the relative velocity of the ejected or accreted matter to the motion of the mass-losing or accreting body.

In this section, we derived the phase-dependent time evolution equations of the orbital elements for non-conservative mass transfer assuming point masses. In Paper II, we orbit-average these equations and derive the secular time evolution equations of the orbital elements under the point-mass approximation and for some commonly used characteristic examples of mass loss/transfer in the adiabatic regime.

8. CONCLUSIONS

Motivated by observations of many mass-transferring eccentric binary systems, in this paper, we derive self-consistent equations for the orbital evolution of interacting eccentric binaries.

We presented a general formalism to derive the time evolution equations of the orbital elements of a binary exposed to general perturbations. We applied this formalism to the case of mass loss and mass transfer in a binary, treating the latter as perturbations to the general two-body problem. We first discussed the cases of isotropic and anisotropic wind mass loss. We then studied the general case of non-isotropic ejection and accretion in a conservative as well as a non-conservative manner for both point masses and extended bodies.

The main results of the paper are summarized below.

1. We discussed the physical interpretation of the osculating orbital elements within the context of gauge freedom in celestial mechanics. We presented two different ways to derive the phase-dependent time evolution equations of the orbital elements and commented on the advantages of each method.
2. We pointed out the importance of the choice of reference frame since an incorrect treatment can lead to misinterpretations of the orbital evolution of the system. We derived the phase-dependent time evolution equations of the semimajor axis and eccentricity in three different reference frames, pointing out the importance of using the right set of time evolution equations for the chosen reference frame. Through comparison with other work in the literature, we presented the necessary corrections that have to be made so that the chosen set of time evolution equations of the orbital elements is consistent with the chosen reference frame in the problem.
3. For completeness, we studied the case of isotropic wind mass loss. We verified that for isotropic mass loss, the semimajor axis as well as the periastron position can never decrease throughout the orbit. On the contrary, the eccentricity undergoes oscillations on orbital timescales. The amplitude of these oscillations is proportional to the ratio of the orbital period to the mass loss timescale and increases over time.
4. We considered the case of anisotropic wind mass loss. Under the assumption of phase-independent anisotropic wind mass loss the orbital evolution depends on the velocity and structure of the stellar wind along the surface and relative to the center-of-mass of the mass-losing body. By making use of the correct transformation treatment between different reference frames that we described in a previous section, we have presented the correct set of time evolution equations of the orbital elements that are necessary to study the case of anisotropic wind mass loss.
5. For either the case of conservative or non-conservative mass transfer for extended bodies, we derived the phase-dependent time evolution equations of the osculating orbital elements. The mass transfer effect on the semimajor axis and eccentricity depends strongly on the binary characteristics and is proportional to the mass loss and mass accretion rates. The mass transfer may either increase or decrease the eccentricity in contrast to tides which always act to circularize the orbit. In the case of extended bodies, the relative ejection and accretion points and associated velocities play an important role as well. Furthermore, in the case of non-conservative mass transfer, there is a strong dependence on the fraction of the total orbital angular momentum the lost mass removes from the system, which in all cases remains a free parameter.
6. The point-mass assumption is often the first approximation to be made in problems regarding mass transfer in binary systems. We presented the form of the time evolution equations of the orbital elements in the non-conservative non-isotropic ejection and accretion case for point masses. We concluded by pointing out the remaining dependence on the relative velocity of the ejected/accreted mass to the motion of the mass-losing/accreting body.

In paper II, we orbit-average the general phase-dependent time evolution equations of the orbital elements presented in this paper. We do so under the assumption of either adiabaticity

or delta-function mass loss/transfer at periastron and for all of the different types of mass loss/transfer studied here. The secular (orbit-averaged) time evolution equations for the semimajor axis and eccentricity are useful analytical equations that can be used to model the evolution of interacting eccentric binaries in star and binary evolution codes like StarTrack (Belczynski et al. 2008), BSE (Hurley et al. 2002), or MESA (Paxton et al. 2011, 2013, 2015).

F.D. and V.K. acknowledge support from grant NSF AST-1517753 and Northwestern University through the "Reach for the Stars" program. The authors also thank our colleagues Dimitri Veras, Jeremy Sepinsky, Michael Efroimsky, and Lorenzo Iorio who provided insight and expertise that greatly assisted the research. We are thankful for their comments that greatly improved the manuscript during its composition and revising stages.

APPENDIX

Using the six Keplerian elements $(a, e, i, \Omega, \omega, \sigma)$ defined in Section 2.1.1, we calculate the partial derivatives of the unperturbed position $\boldsymbol{f}$ and velocity $\boldsymbol{g}$ with respect to the orbital elements, choosing the reference system $K_R(\hat{\boldsymbol{r}}, \hat{\boldsymbol{\tau}}, \hat{\boldsymbol{n}})$ defined in Section 4 and depicted in Figure 3. The unperturbed position and velocity as well as their various partial derivatives with respect to the orbital elements are given as functions of the orbital elements and the true anomaly ν and can be written as follows:

$$(\boldsymbol{f})_r = \frac{a(1-e^2)}{1+e\cos\nu} \tag{125}$$

$$(\boldsymbol{f})_\tau = 0 \tag{126}$$

$$(\boldsymbol{f})_n = 0 \tag{127}$$

$$(\boldsymbol{g})_r = \frac{na}{\sqrt{1-e^2}} e\,\sin\nu \tag{128}$$

$$(\boldsymbol{g})_\tau = \frac{na}{\sqrt{1-e^2}}(1+e\,\cos\nu) \tag{129}$$

$$(\boldsymbol{g})_n = 0 \tag{130}$$

$$\left(\frac{\partial \boldsymbol{f}}{\partial \sigma}\right)_r = \frac{a}{\sqrt{1-e^2}} e\,\sin\nu \tag{131}$$

$$\left(\frac{\partial \boldsymbol{f}}{\partial \sigma}\right)_\tau = \frac{a}{\sqrt{1-e^2}}(1+e\,\cos\nu) \tag{132}$$

$$\left(\frac{\partial \boldsymbol{f}}{\partial \sigma}\right)_n = 0 \tag{133}$$

$$\left(\frac{\partial \boldsymbol{f}}{\partial \omega}\right)_r = 0 \tag{134}$$

$$\left(\frac{\partial \boldsymbol{f}}{\partial \omega}\right)_\tau = \frac{a(1-e^2)}{1+e\cos\nu} \tag{135}$$

$$\left(\frac{\partial \boldsymbol{f}}{\partial \omega}\right)_n = 0 \tag{136}$$

$$\left(\frac{\partial \boldsymbol{g}}{\partial \sigma}\right)_r = -\frac{na}{(1-e^2)^{5/2}}(1+e\,\cos\nu)^2 \tag{137}$$

$$\left(\frac{\partial \boldsymbol{g}}{\partial \sigma}\right)_\tau = 0 \tag{138}$$

$$\left(\frac{\partial \boldsymbol{g}}{\partial \sigma}\right)_n = 0 \tag{139}$$

$$\left(\frac{\partial \boldsymbol{g}}{\partial \omega}\right)_r = -\frac{na}{\sqrt{1-e^2}}(1+e\,\cos\nu) \tag{140}$$

$$\left(\frac{\partial \boldsymbol{g}}{\partial \omega}\right)_\tau = \frac{na}{\sqrt{1-e^2}}(e\,\sin\nu) \tag{141}$$

$$\left(\frac{\partial \boldsymbol{g}}{\partial \omega}\right)_n = 0 \tag{142}$$

$$\left(\frac{\partial \boldsymbol{g}}{\partial a}\right)_r = -\frac{n}{\sqrt{1-e^2}}\sin\nu \tag{143}$$

$$\left(\frac{\partial \boldsymbol{g}}{\partial a}\right)_\tau = \frac{n}{\sqrt{1-e^2}}(1+\cos\nu) \tag{144}$$

$$\left(\frac{\partial \boldsymbol{g}}{\partial a}\right)_n = 0. \tag{145}$$

REFERENCES

Belczynski, K., Kalogera, V., Rasio, F. A., et al. 2008, ApJS, 174, 223
Blandford, R. D., & Payne, D. G. 1982, MNRAS, 199, 883
Boffin, H. M. J., Hillen, M., Berger, J. P., et al. 2014, A&A, 564, A1
Boffin, H. M. J., & Jorissen, A. 1988, A&A, 205, 155
Bogomazov, A. I. 2005, ARep, 49, 709
Bonačić Marinović, A. A., Glebbeek, E., & Pols, O. R. 2008, A&A, 480, 797
Bondi, H., & Hoyle, F. 1944, MNRAS, 104, 273
Boué, G., Figueira, P., Correia, A. C. M., & Santos, N. C. 2012, A&A, 537, L3
Brookshaw, L., & Tavani, M. 1993, ApJ, 410, 719
Church, R. P., Dischler, J., Davies, M. B., et al. 2009, MNRAS, 395, 1127
Davis, P. J., Siess, L., & Deschamps, R. 2014, A&A, 570, A25
de Mink, S. E., Langer, N., Izzard, R. G., Sana, H., & de Koter, A. 2013, ApJ, 764, 166
Dosopoulou, F., & Kalogera, V. 2016, ApJ, arXiv:1603.06593
Efroimsky, M. 2002, Equations for the Keplerian Elements: Hidden Symmetry, Institute for Mathematics and its Applications (Chicago, IL: Univ. of Minnesota Press), 1844
Efroimsky, M., & Goldreich, P. 2003, JMP, 44, 5958
Efroimsky, M., & Goldreich, P. 2004, A&A, 415, 1187
Eggleton, P. P., Kiseleva, L. G., & Hut, P. 1998, ApJ, 499, 853
Flannery, B. P. 1975, MNRAS, 170, 325
Gurfil, P., & Belyanin, S. 2008, AdSpR, 42, 1313
Hadjidemetriou, J. D. 1963, Icar, 2, 440
Huang, S. S. 1956, AJ, 61, 49
Hurley, J. R., Tout, C. A., & Pols, O. R. 2002, MNRAS, 329, 897
Hut, P. 1981, A&A, 99, 126
Lajoie, C.-P., & Sills, A. 2011, ApJ, 726, 67
Meibom, S., & Mathieu, R. D. 2005, ApJ, 620, 970
Omarov, T. B. 1964, SvA, 8, 127
Owocki, S. P., Cranmer, S. R., & Gayley, K. G. 1998, Ap&SS, 260, 149
Paxton, B., Bildsten, L., Dotter, A., et al. 2011, ApJS, 192, 3
Paxton, B., Cantiello, M., Arras, P., et al. 2013, ApJS, 208, 4
Paxton, B., Marchant, P., Schwab, J., et al. 2015, ApJS, 220, 15
Petrova, A. V., & Orlov, V. V. 1999, AJ, 117, 587
Raguzova, N. V., & Popov, S. B. 2005, A&AT, 24, 151
Regös, E., Bailey, V. C., & Mardling, R. 2005, MNRAS, 358, 544
Sepinsky, J. F., Willems, B., Kalogera, V., & Rasio, F. A. 2007, ApJ, 667, 1170
Sepinsky, J. F., Willems, B., Kalogera, V., & Rasio, F. A. 2009, ApJ, 702, 1387
Sepinsky, J. F., Willems, B., Kalogera, V., & Rasio, F. A. 2010, ApJ, 724, 546

Soberman, G. E., Phinney, E. S., & van den Heuvel, E. P. J. 1997, A&A, 327, 620
Soker, N. 2000, A&A, 357, 557
Veras, D., Hadjidemetriou, J. D., & Tout, C. A. 2013, MNRAS, 435, 2416
Veras, D., Wyatt, M. C., Mustill, A. J., Bonsor, A., & Eldridge, J. J. 2011, MNRAS, 417, 2104
Vos, J., Østensen, R. H., Degroote, P., et al. 2012, A&A, 548, A6
Vos, J., Østensen, R. H., Marchant, P., & Van Winckel, H. 2015, A&A, 579, A49
Vos, J., Østensen, R. H., Németh, P., et al. 2013, A&A, 559, A54
Walter, R., Lutovinov, A. A., Bozzo, E., & Tsygankov, S. S. 2015, A&ARv, 23, 2